Fractional atomic coordinates and thermal parameters for **1** and **2** are listed in Tables IV and V, while some relevant interatomic distances and angles are reported in Table VI. Additional details, including a full presentation of data collection parameters and refinement information, nonessential bond distances and angles, least-squares planes, and tables of structure factors, are available as supplementary material. The SHELXTL-PLUS package of computer programs was employed for the solution and refinement of the structures.[18]

(18) Sheldrick, G. M. SHELXTL-PLUS. An Integrated System for Solving, Refining and Displaying Crystal Structures from Diffraction Data For Nicolet R3m/V. University of Göttingen, Germany, 1987.

Acknowledgment. Parke-Davis is gratefully acknowledged for a research grant to G.T. We thank the Progetto Finalizzato Chimica Fine II, CNR, for partial support.

Supplementary Material Available: For **1** and **2**, Table A, containing a full presentation of data collection parameters and refinement information, Tables B-D, listing bond distances and angles, least-squares planes, deviations of the relevant atoms, and dihedral angles, Figure A, showing another perspective view of **1**, Figure B, showing a packing diagram of **2**, and Figure C, showing superimposition of the cations of **1** and **2** (8 pages); Tables E and F, listing observed and calculated structure factors for both compounds (19 pages). Ordering information is given on any current masthead page.

Contribution from the Department of Chemistry and Biochemistry, University of Notre Dame, Notre Dame, Indiana 46556

Electron-Transfer Reactions of Bis(dipeptide)nickel(III) Complexes

Steven E. Schadler, Christopher Sharp, and A. Graham Lappin*

Received May 22, 1991

The kinetics and mechanism of the oxidation of $[Co(edta)]^{2-}$ ($edta^{4-}$ = 1,2-diaminoethane-*N*,*N*,*N*′,*N*′-tetraacetate(4−)) by four bis(dipeptide)nickel(III) complexes, $[Ni(H_{-1}GG)_2]^-$, $[Ni(H_{-1}GA)_2]^-$, $[Ni(H_{-1}AG)_2]^-$, and $[Ni(H_{-1}AA)_2]^-$ (GH = glycine, AH = (*S*)-alanine), have been investigated at 25.0 °C and in 0.10 M perchlorate media. The reactions are first order in each reagent and have a complex dependence on pH. The dominant pathway over the pH range 4–10 involves the acid-catalyzed formation of a precursor complex through which electron transfer takes place. Structural information on the intermediate has been obtained from ^1H NMR relaxation studies of the diamagnetic analogue $[Co(H_{-1}AA)_2]^-$ in the presence of the paramagnetic probe $[Cr(edta)]^-$. There is indirect evidence for a strong hydrogen-bonding interaction between the N-terminal amine hydrogen atoms of a coordinated dipeptide ligand and the carboxylate oxygen atoms of the probe complex. The bis(dipeptide) ligands are arranged meridionally around the nickel(III) to produce a chiral center, and the complexes with optically active dipeptides exist as diastereomers which are readily separated by chromatography. Spectroscopic properties are reported. Stereoselectivity in the reaction with $[Co(edta)]^{2-}$ has been investigated with these complexes, and the results are interpreted in light of the structure of the proposed intermediate.

Introduction

Over the past decade there have been a number of reports of stereoselectivity in electron-transfer reactions between chiral metal complexes.[1-5] In general, stereoselectivities are not large but have proved useful in suggesting structures for intermediates in the electron-transfer process, an important component of mechanism which complements kinetic information. Despite the availability of chiral structures in biological systems, few studies of electron-transfer stereoselectivity involving complexes with biological ligands have been published. The unusually long-lived complexes[6,7] of nickel(III) $[Ni(H_{-1}GG)_2]^-$ (GGH = glycylglycine) and related analogues with optically active dipeptides $[Ni(H_{-1}GA)_2]^-$, $[Ni(H_{-1}AG)_2]^-$, and $[Ni(H_{-1}AA)_2]^-$ (AH = (*S*)-alanine) are of particular interest as chiral oxidants. Structural data are available for the corresponding nickel(II) complexes[8,9] and reveal that the dipeptide ligands are tridentate chelates coordinated meridionally in the high-spin d^8 complexes and are related by a C_2 axis. EPR evidence for the low-spin d^7 nickel(III) analogues indicates a similar coordination geometry.[6] The complex $[Ni(H_{-1}GG)_2]^-$ is chiral (Figure 1), and the enantiomers are designated P(C_2) and M(C_2), where P and M refer to plus (clockwise) and minus (anticlockwise) helicity around the C_2 axis, respectively. For the complexes with optically active dipeptides, the isomers are diastereomers.

The reduction potential[6] of $[Ni(H_{-1}GG)_2]^-$ is sufficiently large to oxidize $[Co(edta)]^{2-}$, a useful probe[1,3,5] for electron-transfer stereoselectivity, and preliminary studies of stereoselectivity in the reaction between the optically active complex $[Ni(H_{-1}AA)_2]^-$ and $[Co(edta)]^{2-}$ were sufficiently encouraging to merit a more complete investigation. Stereoselectivity in this reaction is of particular interest since it involves electron transfer between two anionic complexes which experience electrostatic repulsions.

Experimental Details

(a) Materials. Metal perchlorate salts, $Ni(ClO_4)_2$, $Co(ClO_4)_2$, and $NaClO_4$, were obtained from commercial sources (Alfa and Baker "Analyzed") or were prepared from the corresponding metal carbonate and perchloric acid and were recrystallized before use. The dipeptide ligands glycylglycine, (*S*)-glycylalanine, (*S*)-alanylglycine, and (*S*,*S*)-alanylalanine (all Sigma) were used without further purification. Solutions of $[Ni(H_{-1}GG)_2]^{2-}$ ($\approx 10^{-3}$ M) were prepared by the slow addition of NaOH to a solution of $Ni(ClO_4)_2$ containing a 5-fold excess of the GGH to pH 11. The resulting pale blue solution of $[Ni(H_{-1}GG)_2]^{2-}$ was filtered and oxidized to the deep violet $[Ni(H_{-1}GG)_2]^-$ by controlled-potential electrolysis at 850 mV with use of a flow cell comprising a charcoal working electrode packed in a 70 × 7 mm Vycor glass column, a platinum-wire counter electrode, and a Ag/AgCl reference with 0.10 M $NaClO_4$ as electrolyte.[10] A PAR Model 173 potentiostat was used to supply the voltage which was measured relative to the reference

(1) Geselowitz, D. A.; Taube, H. *J. Am. Chem. Soc.* **1980**, *102*, 4525-4526.
(2) Kondo, S.; Sasaki, Y.; Saito, K. *Inorg. Chem.* **1981**, *20*, 429-433.
(3) Osvath, P.; Lappin, A. G. *Inorg. Chem.* **1987**, *26*, 195-202.
(4) Marusak, R. A.; Osvath, P.; Kemper, M.; Lappin, A. G. *Inorg. Chem.* **1989**, *28*, 1542-1548.
(5) Marusak, R. A.; Lappin, A. G. *Coord. Chem. Rev.* **1991**, *109*, 125-180.
(6) Jacobs, S. A.; Margerum, D. W. *Inorg. Chem.* **1984**, *23*, 1195-1201.
(7) Anliker, S. L.; Beach, M. W.; Lee, H. D.; Margerum, D. W. *Inorg. Chem.* **1988**, *27*, 3809-3818.
(8) Freeman, H. C.; Guss, J. M.; Sinclair, R. L. *J. Chem. Soc., Chem. Commun.* **1968**, 485-487.
(9) Freeman, H. C.; Guss, J. M. *Acta Crystallogr.* **1978**, *B34*, 2451-2458.
(10) Clark, B. R.; Evans, D. H. *J. Electroanal. Chem. Interfacial Electrochem.* **1976**, *69*, 181-184.

0020-1669/92/1331-0051$03.00/0

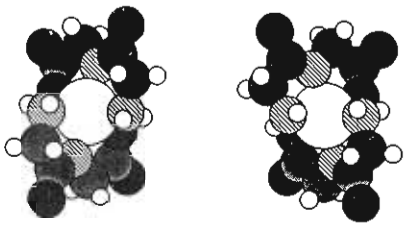

M(C_2) P(C_2)

Figure 1. View down the N-terminal C_2 axis of $[Ni(H_{-1}GG)_2]^-$, showing the P(C_2) (clockwise) and M(C_2) (anticlockwise) helical arrangement of the ligands. Amine nitrogens are striped, carbons are shaded, and oxygens are black.

electrode. Solutions of the other nickel(III) complexes $[Ni(H_{-1}GA)_2]^{2-}$, $[Ni(H_{-1}AG)_2]^{2-}$, and $[Ni(H_{-1}AA)_2]^{2-}$ were obtained by similar procedures at potentials 700, 650, and 600 mV, respectively. The nickel(III) complexes were purified immediately before use on QAE-Sephadex resin (10 × 1 cm, Q-25-120, Sigma), eluting with 0.10 M sodium perchlorate, and the concentration was determined spectrophotometrically (ϵ_{560} = 500 M^{-1} cm^{-1}).[11] Separation of the diastereomers of complexes of the optically active bis(dipeptide) ligands was accomplished on a water-jacketed QAE-Sephadex column (40 × 1 cm) thermostated at 4 °C with 0.020 M $NaClO_4$ as eluent.

Solutions of $[Co(edta)]^{2-}$ were prepared from cobalt(II) perchlorate with a 5% excess of Na_2H_2edta and were standardized spectrophotometrically. Solutions of $[Co(phen)_3]^{2+}$ were prepared from cobalt(II) nitrate (Baker Analyzed) and 1,10-phenanthroline (Fluka) in sufficient excess to ensure >99% formation of the tris complex.[12] The preparation of $[Co(H_{-1}AA)_2]^-$ was accomplished by the literature procedure.[13] Separation of the diastereomers was carried out on QAE-Sephadex resin with 0.020 M $NaClO_4$ as eluent at 25.0 °C, and the separated diastereomers were desalted on a G-10 Sephadex column (Sigma G-10-120; ~50 × 1 cm). The complex $[Cr(edta)]^-$ was prepared as described in the literature.[14,15]

(b) Methods. The stoichiometry of the reaction between $[Ni(H_{-1}GG)_2]^-$ and $[Co(edta)]^{2-}$ was determined spectrophotometrically at 560 nm by measuring the amount of $[Ni(H_{-1}GG)_2]^-$ consumed when less than stoichiometric amounts of the reductant were added to a standardized solution. These studies were complemented by quantitative recovery of the $[Co(edta)]^-$ product formed when an excess (×50) of $[Co(edta)]^{2-}$ was added to a standard solution of 1.7 × 10^{-4} M $[Ni(H_{-1}GG)_2]^-$. Reaction mixtures were acidified and diluted, and the cobalt(III) product was isolated on QAE-Sephadex or Amberlite CG-400 anion-exchange resin, washed with 10^{-4} M HCl, and eluted with 0.1 M HCl. The immediate nickel(II) product was not isolated, since rapid hydrolysis ensues. The kinetics of the reduction of the bis(dipeptide)-nickel(III) complexes were observed at 560 nm under pseudo-first-order conditions with a nickel(III) concentration ≈ 10^{-4} M and greater than a 10-fold excess of reductant at 25.0 °C and 0.10 M ionic strength. In some experiments, atmospheric oxygen was rigorously excluded by purging with Ar gas but this was found to have no effect on the reaction. The supporting electrolyte for $[Co(edta)]^{2-}$ as reductant was $NaClO_4$ and for $[Co(phen)_3]^{2+}$ was $NaNO_3$. Buffers, *N*-morpholineethanesulfonic acid (MES), *N*-(2-hydroxyethyl)piperazine-*N*'-ethanesulfonic acid (HEPES), tris(hydroxymethyl)aminomethane (TRIS), 3-(cyclohexylamino)-1-propanesulfonic acid (CAPS), 3-(cyclohexylamino)-2-hydroxy-1-propanesulfonic acid (CAPSO), acetate, chloroacetate, and borate (Sigma or Baker "Analyzed"), were used at concentrations of 0.01 M. All pH measurements were made with a Beckman SelectIon 2000 pH meter equipped with a Corning semimicro combination electrode using a sodium chloride reference. Kinetic measurements were made with use of a Varian DMS 100 spectrophotometer for slower reactions or a Durrum D-110 stopped-flow spectrophotometer for faster reactions. Data were collected using a Macintosh SE computer and a GW Instruments MacADIOS data aquisition system. Plots of ln ($A - A_\infty$) against time were generally linear for at least 3 half-lives, and the pseudo-first-order rate constants, k_{obsd}, were evaluated from the slopes by linear least-squares procedures.

Stereoselectivity in the reaction with $[Co(edta)]^{2-}$ was measured at 0.10 M ionic strength and 23 °C with nickel(III) concentrations around 10^{-3} M and an excess of reductant. After acidification to pH 4 and dilution of the reaction mixture, the $[Co(edta)]^-$ product was isolated chromatographically on QAE-Sephadex resin and optical activity determined. In some experiments it was found possible to determine the optical activity of the $[Co(edta)]^-$ by direct measurement on the reaction mixture. Both methods gave excellent agreement. Circular dichroism spectra were run on an Aviv Model 60DS circular dichroism spectrophotometer (Aviv Associates, Lakewood, NJ). The absolute configuration is Δ-$[(+)_{546}$-$Co(edta)]^-$ ($\Delta\epsilon_{575}$ = −1.79 M^{-1} cm^{-1}).[16] Similar experiments were carried out with $[Co(phen)_3]^{2+}$ as reductant. However, due to the rapid self-exchange racemization of $[Co(phen)_3]^{3+}$ in the presence of excess $[Co(phen)_3]^{2+}$, the circular dichroism was determined at 487 nm directly on the reaction mixture by use of a rapid-mixing flow technique.[17] The absolute configuration is Δ-$[(+)_{589}$-$Co(phen)_3]^{3+}$ ($\Delta\epsilon_{487}$ = 1.19 M^{-1} cm^{-1}).[18]

NMR spectra and T_1 relaxation experiments were performed on a Nicolet NT300 300-MHz NMR spectrometer at 25 °C. The concentration of $[Co(H_{-1}AA)_2]^-$ was ≈10^{-1} M, and the $[Cr(edta)]^-$ concentration was varied from 1.4 × 10^{-3} to 4.4 × 10^{-3} M. The complexes, in D_2O solution, were recrystallized from D_2O (×3) prior to use, and solutions were thoroughly purged with argon prior to use. The technique employed was an inversion-recovery program which used a 180°–τ–90° pulse sequence, where τ is a delay time. At least 12 τ values were used in each experiment, and $1/T_1$ was evaluated by least-squares analysis from plots of ln ($A_\infty - A_i$) vs τ_i, where A_i is the peak intensity corresponding to τ_i and A_∞ is the intensity of the completely relaxed peak.

Results

(a) Isolation of Diastereomers. The P(C_2) and M(C_2) isomers for complexes of the optically active dipeptides containing (*S*)-alanine are diastereomers and are readily separated by ion-exchange chromatography. On QAE-Sephadex resin with 0.10 M sodium perchlorate as eluent, complete separation of the isomers of $[Ni(H_{-1}AA)_2]^-$ into two distinct bands was achieved. The visible and circular dichroism spectra are shown in Figure 2. Only partial separation was observed for $[Ni(H_{-1}GA)_2]^-$, and samples of the diastereomers were obtained by collecting leading and trailing edges of the band. Comparisons of the molar ellipticities for the samples of $[Ni(H_{-1}GA)_2]^-$ with those for the optically pure $[Ni(H_{-1}AA)_2]^-$, which has similar spectroscopic characteristics, indicate optical purity of these $[Ni(H_{-1}GA)_2]^-$ diastereomeric samples close to 100%. For $[Ni(H_{-1}AG)_2]^-$ no separation of the chromatographic band was observed and the circular dichroism spectra of the leading and trailing edge fractions were identical (Figure 2), leading to the conclusion that a single diastereomer is present in this case. The spectroscopic parameters for the complexes are collected in Table I. Assignment of the absolute configuration for each diastereomer is made on the basis of comparisons with separations of the isostructural cobalt(III) complexes,[13] where the first eluted isomer has the M(C_2) configuration. The circular dichroism spectra for the complexes assigned as M(C_2) all show a dominant negative feature around 325 nm. Significant decomposition of the complexes takes place over a period of 24 h at ambient temperature;[6] however, the circular dichroism spectrum does not change over this period and it decays at the same rate as the visible absorption.

(b) Kinetics of Reaction of $[Ni(H_{-1}GG)_2]^-$ and Derivatives by $[Co(edta)]^{2-}$. The kinetics of the reactions of $[Ni(H_{-1}GG)_2]^-$ and derivatives, $[Ni(H_{-1}GA)_2]^-$, $[Ni(H_{-1}AG)_2]^-$, and $[Ni(H_{-1}AA)_2]^-$, with $[Co(edta)]^{2-}$ have been investigated. All four reactions show similar behavior, and the prototype reaction of $[Ni(H_{-1}GG)_2]^-$ is described in the most detail. All the reactions are complicated by the presence of a number of slowly interconverting isomeric species, as described in the preceding section, and these were not

(11) The values of the extinction coefficients for all four complexes at 560 nm are 500 ± 50 M^{-1} cm^{-1} on the basis of the spectrophotometric titration with ascorbate ion.

(12) McBryde, W. A. E. *IUPAC Chem. Data Ser.* **1978**, *17*, 18–36.
(13) Boas, L. V.; Evans, C. A.; Gillard, R. D.; Mitchell, P. R.; Phipps, D. A. *J. Chem. Soc., Dalton Trans.* **1979**, 582–595.
(14) Sawyer, D. T.; McKinnie, J. M. *J. Am. Chem. Soc.* **1960**, *82*, 4191–4196.
(15) Marusak, R. A.; Sharp, C.; Lappin, A. G. *Inorg. Chem.* **1990**, *29*, 4453–4456.
(16) Gillard, R. D.; Mitchell, P. F.; Weick, C. F. *J. Chem. Soc., Dalton Trans.* **1974**, 1635–1636.
(17) Warren, R. M. L.; Lappin, A. G.; Mehta, B. D.; Neumann, H. M. *Inorg. Chem.* **1990**, *29*, 4185–4189.
(18) Mason, S. F.; Peart, B. J. *J. Chem. Soc., Dalton Trans.* **1973**, 949–955.

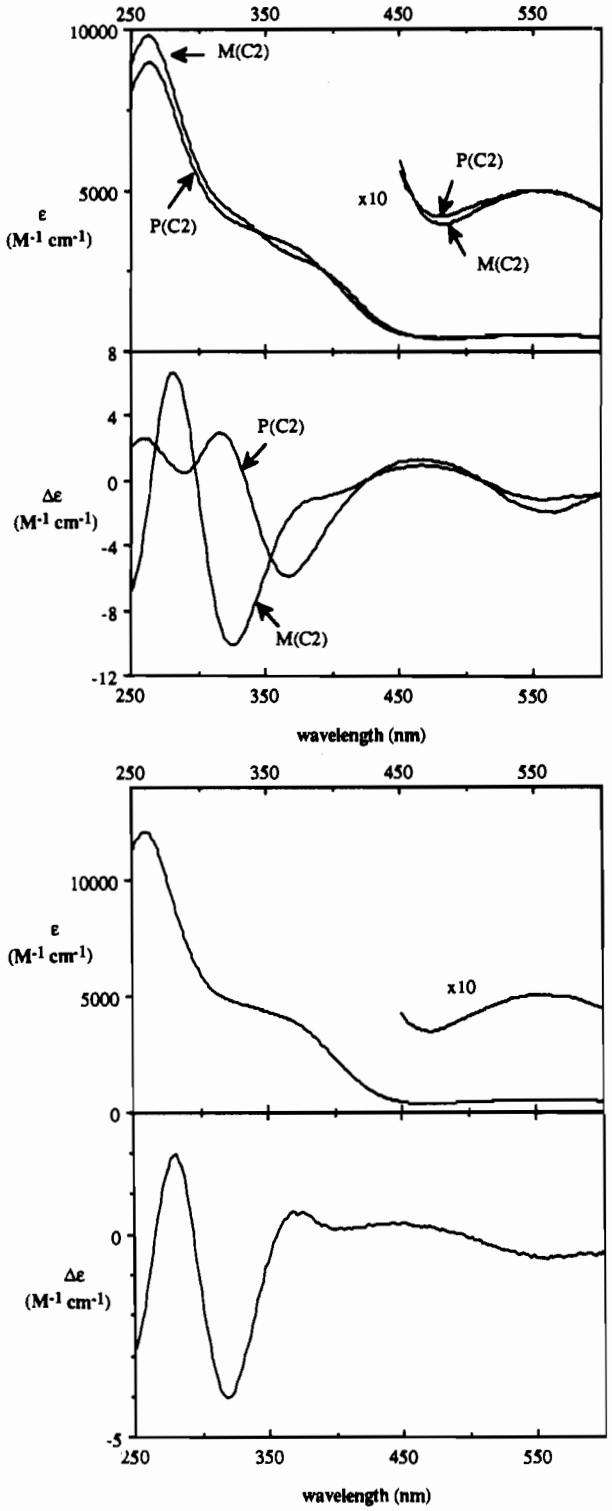

Figure 2. UV–visible and circular dichroism spectra of (a, top) $M(C_2)$- and $P(C_2)$-$[Ni(H_{-1}AA)_2]^-$ and (b, bottom) $M(C_2)$-$[Ni(H_{-1}AG)_2]^-$.

separated for the kinetic studies. Nevertheless, no significant deviations from first-order behavior due to this heterogeneity were recognized and it is likely that enantiomers and diastereomers for any particular complex have similar reactivities. The small magnitudes of the chiral inductions observed in these reactions support this point. These inductions would be difficult to detect by kinetic measurements.

In the reaction, $[Co(edta)]^{2-}$ is oxidized to $[Co(edta)]^-$ and the nickel complex is reduced to a labile product which is rapidly hydrolyzed and was not isolated. The stoichiometry, determined by the amount of $[Co(edta)]^-$ isolated, is 0.98 ± 0.04 mol of $[Co(edta)]^{2-}$ consumed/mol of $[Ni(H_{-1}GG)_2]^-$, consistent with eq 1. Spectrophotometric measurements in the presence of an excess of $[Ni(H_{-1}GG)_2]^-$ indicate a stoichiometry of 0.95:1.00, also in good agreement.

$$[Ni(H_{-1}GG)_2]^- + [Co(edta)]^{2-} \rightarrow [Ni(H_{-1}GG)_2]^{2-} + [Co(edta)]^- \quad (1)$$

Under pseudo-first-order conditions with an excess of $[[Co(edta)]^{2-}]$, the rate of reduction of $[Ni(H_{-1}GG)_2]^-$, measured at 560 nm, shows good first-order behavior for at least 3 half-lives. Above pH 4, plots of the pseudo-first-order rate constants, k_{obsd}, against $[[Co(edta)]^{2-}]$ are linear with intercepts which are negligible within experimental error, indicating a first-order dependence on $[[Co(edta)]^{2-}]$. Below pH 4, the acid-catalyzed decomposition of $[Ni(H_{-1}GG)_2]^-$, k_H, contributes significantly to the rate and the first-order rate constants were corrected with use of the relationship $k_{corr} = k_{obsd} - k_H$. Some values of k_H were measured experimentally and showed excellent agreement with those reported in the literature;[6] otherwise literature values were used to correct the data. Pseudo-first-order rate constants, k_{obsd}, obtained under a variety of conditions are presented in Table SI, available as supplementary material.

Second-order rate constants for the electron transfer, k_{so}, show a complex dependence on pH (Figure 3). Between pH 5 and 8, the rate is independent of pH with a second-order rate constant which averages 24.3 ± 0.8 M^{-1} s^{-1}. Below this pH the rate increases sharply. A dependence of this sort is not unexpected at both reagents are known to undergo protonation at lower pH.

Table I. Visible and Circular Dichroism Spectroscopic Parameters for Bis(dipeptide)nickel(III) Complexes in Aqueous Solution at 25.0 °C

complex	λ, nm	ε, M^{-1} cm^{-1}	Δε, M^{-1} cm^{-1}
$M(C_2)$-$[Ni(H_{-1}GA)_2]^-$	560	500	
	558		−0.86
	474		0.92
	395 (sh)	3000	
	380		−1.1
	326		−10.1
	283		7.12
	262	10600	
$P(C_2)$-$[Ni(H_{-1}GA)_2]^-$	560	500	
	558		−0.75
	482		0.72
	366		−5.1
	365 (sh)	4400	
	320		2.3
	294		−0.30
	262	11400	
	260		3.59
$M(C_2)$-$[Ni(H_{-1}AG)_2]^-$	560	500	
	558		−0.70
	452		0.28
	400		0.11
	375 (sh)	3700	
	374		0.55
	318		−4.1
	282		1.95
	261	12000	
$M(C_2)$-$[Ni(H_{-1}AA)_2]^-$	560	500	
	558		−1.3
	470		0.88
	390 (sh)	2600	
	380		−1.2
	340 (sh)	3900	
	324		−10.0
	282		6.66
	263	9800	
$P(C_2)$-$[Ni(H_{-1}AA)_2]^-$	560	500	
	558		−1.9
	472		1.2
	375 (sh)	3200	
	370		−5.4
	318		2.9
	290		0.43
	265	9000	
	262		2.58

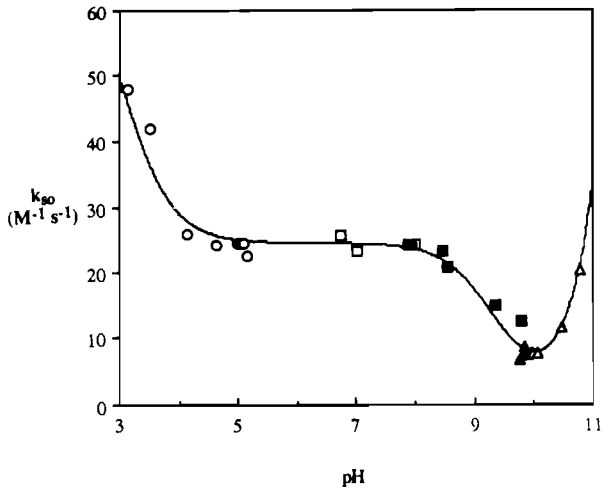

Figure 3. Plot of the second-order rate constant for the reduction of $[Ni(H_{-1}GG)_2]^-$ by $[Co(edta)]^{2-}$ as a function of pH at 25.0 °C and 0.10 M ionic strength. The buffers used are acetate (open circles), TRIS (open squares), HEPES (filled circles), borate (filled squares), CAPSO (filled triangles), and CAPS (open triangles). The solid line is a fit of the data to eq 9.

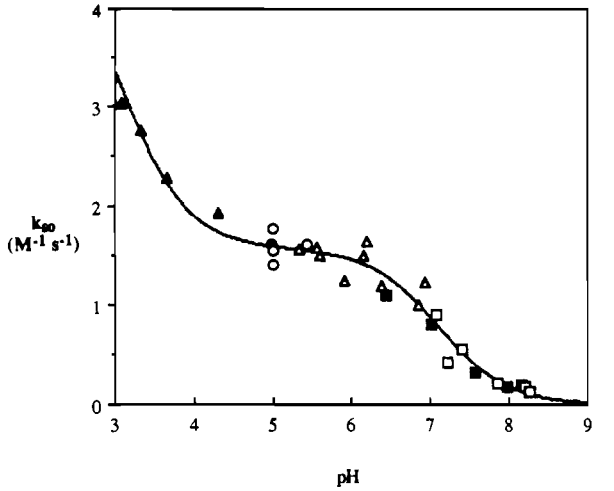

Figure 4. Plot of the second-order rate constant for the reduction of $[Ni(H_{-1}AA)_2]^-$ by $[Co(edta)]^{2-}$ as a function of pH at 25.0 °C and 0.10 M ionic strength. The buffers used are chloroacetate (filled triangles), acetate (open circles), TRIS (open squares), HEPES (filled squares), and MES (open triangles). The solid line is a fit of the data to eq 9.

The reductant, $[Co(edta)]^{2-}$, has a pK_{a1} around 3.0,[19] and the $[Ni(H_{-1}GG)_2]^-$ complex shows evidence for outside protonation in this pH range,[6] although pK_a values are not known. Because of the complications of the acid-catalyzed decomposition of $[Ni(H_{-1}GG)_2]^-$ and to simplify the analysis of the reaction, a single $[H^+]$-dependent pathway (eqs 2 and 3) was considered and found

$$[Co(Hedta)]^- \overset{K_{a1}}{\rightleftharpoons} [Co(edta)]^{2-} + H^+ \qquad K_{a1} = 1.0 \times 10^{-3}\ M \tag{2}$$

$$[Ni(H_{-1}GG)_2]^- + [Co(Hedta)]^- \xrightarrow{k_a} [Ni(H_{-1}GG)_2]^{2-} + [Co(edta)]^- + H^+ \tag{3}$$

to be sufficient to explain the limited data which were collected, with $k_a = 75 \pm 5\ M^{-1}\ s^{-1}$. It is above pH 8, however, that the most interesting behavior is observed. There is an initial decrease in rate between pH 8 and 10 followed by an increase above pH 10, so that at least two proton-dependent processes are involved. There is some evidence from the product analysis that $[Co(edta)OH]^{2-}$ is formed at pH ≥10. Addition of OH^- to $[Co(edta)]^{2-}$ is reported[20] with pK_b 0.83, and this can account for the increase in rate above pH 10 (eqs 4 and 5), with a rate constant

$$[Co(edta)]^{2-} \overset{K_{a2}}{\rightleftharpoons} [Co(edta)OH]^{3-} + H^+ \qquad K_{a2} = 6.7 \times 10^{-14} \tag{4}$$

$$[Ni(H_{-1}GG)_2]^- + [Co(edta)OH]^{3-} \xrightarrow{k_b} [Ni(H_{-1}GG)_2]^{2-} + [Co(edta)OH]^{2-} \tag{5}$$

$k_b \approx 5000\ M^{-1}\ s^{-1}$. However, there is no evidence for additional proton-dependent equilibria for either $[Co(edta)]^{2-}$ or $[Ni(H_{-1}GG)_2]^-$ in the pH range 4–11. Spectrophotometric analysis of solutions of the $[Ni(H_{-1}GG)_2]^-$ complex over this pH range indicates no change in the position or intensity of the 560-nm band. The complicated pH-dependent behavior is noted with all four oxidants, but the pH at which the rate decreases toward high pH varies with the identity of the nickel(III) complex. The effect is independent of buffer and of the presence of differing amounts of $[H_2edta]^{2-}$ and $[Ni(H_{-1}GG)_2]^{2-}$ added to the solution.

Table II. Rate Parameters for the Reduction of Bis(dipeptide)nickel(III) Complexes by $[Co(edta)]^{2-}$ at 25.0 °C and 0.10 M Ionic Strength ($NaClO_4$)

complex	k_a, $M^{-1}\ s^{-1}$	k_b, $M^{-1}\ s^{-1}$	k_1, $M^{-2}\ s^{-1}$	k_1k_2/k_{-1}, $M^{-1}\ s^{-1}$
$[Ni(H_{-1}GG)_2]^-$	74.9	5000	3.86×10^{10}	24.3
$[Ni(H_{-1}GA)_2]^-$	59.6	2500	3.99×10^{8}	13.9
$[Ni(H_{-1}AG)_2]^-$	22.7	1000	2.30×10^{8}	3.1
$[Ni(H_{-1}AA)_2]^-$	5.14		1.89×10^{7}	1.56
$[Ni(H_{-1}GG)_2]^-$				7300[a]

[a] $[Co(phen)_3]^{2+}$.

In order to pinpoint the source of the pH dependence, and to rule out some previously undetected protic equilibrium of the nickel(III) complex as a possible cause, the reduction of $[Ni(H_{-1}GG)_2]^-$ by the reductant $[Co(phen)_3]^{2+}$ was examined. In this case also, the reaction has 1:1 stoichiometry, and the rate shows a first-order dependence on the concentrations of both reactants. However, there is no significant pH dependence of the second-order rate constant over the range 7.5–10.5. The second-order rate constant, 7300 ± 400 $M^{-1}\ s^{-1}$, is 2 orders of magnitude higher than that for the reaction with $[Co(edta)]^{2-}$, and experiments were carried out with both $[Ni(H_{-1}GG)_2]^-$ and $[Co(phen)_3]^{2+}$ equilibrated in buffer at pH 10 and with the $[Ni(H_{-1}GG)_2]^-$ initially unbuffered and mixed with a buffered solution of $[Co(phen)_3]^{2+}$ at pH 10 to ensure that there was no slow protic equilibrium involving the nickel(III) species which might discriminate between the two reductants.

It can be concluded that while the curious pH dependence in the reaction with $[Co(edta)]^{2-}$ is highly dependent on the nature of the nickel(III) complex, it is not the result of a thermodynamic equilibrium involving this complex alone. Neither is it a thermodynamic equilibrium of some intermediate adduct of $[Ni(H_{-1}GG)_2]^-$ and $[Co(edta)]^{2-}$, since there is no kinetic evidence for the formation of such an adduct as a dominant form of nickel(III) in solution. Nevertheless, the dependence can be satisfactorily explained by the formation of an intermediate, at steady-state concentrations, where the formation reaction is acid catalyzed (eq 6). The intermediate subsequently undergoes

$$[Ni(H_{-1}GG)_2]^- + [Co(edta)]^{2-} + H^+ \overset{k_1}{\underset{k_{-1}}{\rightleftharpoons}} \{[Ni(H_{-1}GG)_2]^-,[Co(edta)]^{2-}\} + H^+ \tag{6}$$

$$\{[Ni(H_{-1}GG)_2]^-,[Co(edta)]^{2-}\} \xrightarrow{k_2} [Ni(H_{-1}GG)_2]^{2-} + [Co(edta)]^- \tag{7}$$

intramolecular electron transfer to the reaction products (eq 7).

(19) Martell, A. E.; Smith, R. M. *Critical Stability Constants*; Plenum: New York, 1974; Vol. 2, p 206.
(20) Bhat, T. R.; Krishnamurthy, M. *J. Inorg. Nuclear Chem.* **1963**, *25*, 1147–1154.

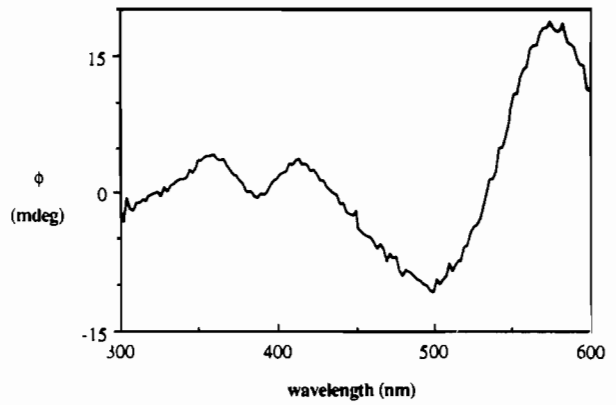

Figure 5. Circular dichroism spectrum of the $[Co(edta)]^-$ product isolated by ion-exchange chromatography from the reaction with $M(C_2)$-$[Ni(H_{-1}AG)_2]^-$ at pH 6.14. The $[Co(edta)]^-$ concentration of the sample is 2.6×10^{-4} M.

Table III. Stereoselectivities Expressed as Enantiomeric Excesses for the Reduction of Bis(dipeptide)nickel(III) Complexes by $[Co(edta)]^{2-}$ at 23.0 °C and 0.10 M Ionic Strength

complex	pH	enantiomeric excess
$M(C_2)$-$[Ni(H_{-1}GA)_2]^-$	6.14	2.0 ± 0.5% Λ
$P(C_2)$-$[Ni(H_{-1}GA)_2]^-$	6.14	12.5 ± 0.5% Δ
$M(C_2)$-$[Ni(H_{-1}AA)_2]^-$	6.10	14.2 ± 0.2% Λ
$P(C_2)$-$[Ni(H_{-1}AA)_2]^-$	6.10	5.9 ± 0.2% Λ
$M(C_2)$-$[Ni(H_{-1}AG)_2]^-$	6.14	14.4 ± 0.2% Λ
$P(C_2)$+$M(C_2)$-$[Ni(H_{-1}GA)_2]^-$	6.11	6.9 ± 0.5% Δ
$P(C_2)$+$M(C_2)$-$[Ni(H_{-1}GA)_2]^-$	3.67	6.9 ± 0.5% Δ
$M(C_2)$-$[Ni(H_{-1}AG)_2]^-$	3.70	14.0 ± 0.4% Λ
$P(C_2)$+$M(C_2)$-$[Ni(H_{-1}GA)_2]^-$	10.14	5.5 ± 0.5% Δ
$M(C_2)$-$[Ni(H_{-1}AG)_2]^-$	10.17	3.5 ± 0.5% Λ

Best fit rate parameters are $k_1 = (3.9 \pm 0.5) \times 10^{10}$ M^{-2} s^{-1} and $k_1k_2/k_{-1} = 24.3 \pm 0.8$ M^{-1} s^{-1}. The subsequent rate law (eq 8)

$$-d[[Ni(H_{-1}GG)_2]^-]/dt = \{k_1k_2[H^+]/\{k_{-1}[H^+] + k_2\}\}[[Ni(H_{-1}GG)_2]^-][[Co(edta)]^{2-}] \quad (8)$$

$$k_{so} = \frac{\{k_a[H^+]^2 + K_{a1}k_1k_2[H^+]^2/\{k_{-1}[H^+] + k_2\} + k_bK_{a1}K_{a2}\}}{\{[H^+]^2 + K_{a1}[H^+] + K_{a1}K_{a2}\}} \quad (9)$$

gives the desired dependence on pH and combined with the pathways eqs 2–5 gives the overall second-order rate constant (eq 9). The fit to this equation for the reactions with $[Ni(H_{-1}GG)_2]^-$ and $[Ni(H_{-1}AA)_2]^-$ is shown in Figures 3 and 4, respectively, and the derived rate and equilibrium constant are summarized in Table II.

(c) Stereoselectivity Studies. From the separations of the diastereomers of the complexes with optically active dipeptides, five chiral complexes, $M(C_2)$-$[Ni(H_{-1}GA)_2]^-$, $P(C_2)$-$[Ni(H_{-1}GA)_2]^-$, $M(C_2)$-$[Ni(H_{-1}AA)_2]^-$, $P(C_2)$-$[Ni(H_{-1}AA)_2]^-$, and $M(C_2)$-$[Ni(H_{-1}AG)_2]^-$, are obtained in solutions of high optical purity. These chiral complexes react with the enantiomers of labile $[Co(edta)]^{2-}$ at slightly different rates resulting in the induction of optical activity in the inert $[Co(edta)]^-$ product. The circular dichroism spectrum of the $[Co(edta)]^-$ product isolated by ion-exchange chromatography from the reaction with $M(C_2)$-$[Ni(H_{-1}AG)_2]^-$ run at pH 6.14 is shown in Figure 5. The Λ form is in enantiomeric excess and is calculated to be 14.4% optically pure. Results for all the complexes under these conditions are presented in Table III. Data as a function of changing pH were obtained for a diastereomeric mixture of $M(C_2)$-$[Ni(H_{-1}GA)_2]^-$ and $P(C_2)$-$[Ni(H_{-1}GA)_2]^-$ and for the single isomer $M(C_2)$-$[Ni(H_{-1}AG)_2]^-$, which does not require separation of the diastereomers. In both cases, values at pH 3.7 and 6.1 are comparable and are significantly higher than the value obtained at pH 10.1, where the product initially formed after acidification is a mixture of both $[Co(edta)]^-$ and $[Co(edta)(H_2O)]^-$.[21]

Table IV. Relaxation Rates ($1/T_1$) and Slopes (Relaxivities) from Plots of $1/T_1$ against $[[Cr(edta)]^-]$ for ^1H in $M(C_2)$- and $P(C_2)$-$[Co(H_{-1}AA)]^-$ at 25.0 °C

$10^3[[Cr(edta)]^-]$, M	$1/T_1$-$(C(CH_3))$,[a] s^{-1}	$1/T_1$-$(N(CH_3))$,[b] s^{-1}	$1/T_1$-$(C(CH))$,[c] s^{-1}	$1/T_1$-$(N(CH))$,[d] s^{-1}
		$M(C_2)$		
0.00	1.82	2.26	0.59	0.74
1.36	3.43	5.39	2.85	5.77
2.53	4.01	7.36	5.52	13.2
3.54	5.19	10.6	6.64	16.8
4.43	6.59	12.4	11.7	19.7
relaxivity, M^{-1} s^{-1}	**1020**	**2290**	**2320**	**4450**
		$P(C_2)$		
0.00	1.75	2.16	0.66	0.70
1.36	3.73	5.61	2.03	3.13
2.53	5.72	8.1	3.48	5.59
3.54	7.66	10.7	4.88	7.84
4.43	9.1	12.6	6.12	9.6
relaxivity, M^{-1} s^{-1}	**1780**	**2360**	**1240**	**2030**

[a] C-terminal methyl resonance. [b] N-terminal methyl resonance. [c] C-terminal methine resonance. [d] N-terminal methine resonance.

(d) ^1H NMR Relaxation Experiments. The evidence from the kinetic studies for a well-defined intermediate in the reaction between $[Ni(H_{-1}GG)_2]^-$ and $[Co(edta)]^{2-}$ suggests that structural information on this species may be important for understanding the mechanism and interpretation of the stereoselectivity. In previous work,[22] paramagnetic relaxation experiments have provided valuable information on the structures of labile ion pairs. To facilitate the investigation, the complex $[Co(H_{-1}AA)_2]^-$ was used as a diamagnetic analogue for $[Ni(H_{-1}GG)_2]^-$ and the interaction of this complex with $[Cr(edta)]^-$, a paramagnetic analogue for $[Co(edta)]^{2-}$, was investigated. The $[Co(H_{-1}AA)_2]^-$ complex was chosen because the four observable proton environments in the ^1H NMR spectrum are readily identified and assigned.[13] Both diastereomers of $[Co(H_{-1}AA)_2]^-$ were prepared, and the details of the ^1H NMR spectra of the complexes are presented in Table IV.

For inert, diamagnetic species such as $[Co(H_{-1}AA)_2]^-$, ^1H NMR relaxation times (T_1) are determined primarily by the rate of tumbling of the complexes in solution. However, in a structured ion pair with the paramagnetic ion $[Cr(edta)]^-$, the relaxation times are reduced according to eq 10. In this equation, M_{diam}

$$(1/T_1)_{obsd} = M_{diam}(1/T_1)_{diam} + M_{para}(1/T_1)_{para} \quad (10)$$

is the mole fraction of $[Co(H_{-1}AA)_2]^-$ free in solution and M_{para} is the mole fraction in the structured ion pair; $(1/T_1)_{diam}$ is the relaxation rate in the absence of the paramagnetic ion and $(1/T_1)_{para}$ is the relaxation rate in the isolated structured ion pair. The equilibrium constant for formation of the ion pair, K, is small, and consequently, in the presence of a large excess of the diamagnetic complex, eq 10 can be modified to eq 11. Additional

$$(1/T_1)_{obsd} = (1/T_1)_{diam} + \{K/(1 + K[Co(III)]_T)\}(1/T_1)_{para}[[Cr(edta)]^-] \quad (11)$$

contributions to the relaxivities from unstructured interactions will also occur, and these will also show a linear dependence on $[[Cr(edta)]^-]$.[22] The dependencies of $(1/T_1)_{obsd}$ on $[[Cr(edta)]^-]$ for the four ^1H environments in $M(C_2)$-$[Co(H_{-1}AA)_2]^-$ and $P(C_2)$-$[Co(H_{-1}AA)_2]^-$ are linear, in good agreement with eq 11. Furthermore, the slopes of the lines, or relaxivities, show a strong dependence on the position of the ^1H on the ligand backbone (Table IV), a characteristic of well-structured ion-pairing inter-

(21) The circular dichroism spectrum of Λ-$(-)_{546}$-*cis*-eq-$[Co(Hedta)(H_2O)]$, $\Delta\epsilon_{584} = +0.23$ M^{-1} cm^{-1} and $\Delta\epsilon_{529} = -1.02$ M^{-1} cm^{-1} (Russell, R. L. Ph.D. Thesis, University of Pittsburgh, 1970. Quoted in: Radanovic, D. J. *Coord. Chem. Rev.* **1984**, *54*, 159–261) is characteristically different from that of Λ-$(-)_{546}$-$[Co(edta)]^-$, $\Delta\epsilon_{575} = +1.79$ M^{-1} cm^{-1} and $\Delta\epsilon_{500} = -0.83$ M^{-1} cm^{-1}.[16]

(22) Marusak, R. A.; Lappin, A. G. *J. Phys. Chem.* **1989**, *93*, 6856–6859.

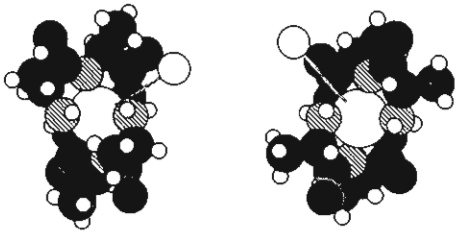

Figure 6. View down the C_2 axes of $M(C_2)$- and $P(C_2)$-$[Co(H_{-1}AA)_2]^-$, showing the position of the paramagnetic center of $[Cr(edta)]^-$ in the structured ion pair as deduced from ^1H NMR relaxation experiments. Note the position of the N-terminal amine hydrogen atoms, which are thought to participate in hydrogen bonding. Note also that the paramagnetic center is distorted away from the methyl substituents in the $P(C_2)$ isomer.

actions. The coordinates of the paramagnetic center were adjusted until a correlation coefficient >0.9999 was obtained for a plot of $(1/T_1)_{obsd}$ against $(1/N)\sum(1/r_i^6)$, where r_i is the distance between the paramagnetic center and the ith equivalent proton of the cobalt(III) complex and N is the number of equivalent proton environments in the complex. For each system, the ion-pairing constant, K, remains constant, and this procedure optimizes the Solomon–Bloembergen[23,24] correlation between $\{K/(1 + K[Co(III)]_T)\}(1/T_1)_{para}$ and $(1/N)\sum(1/r_i^6)$. The component of the relaxivity which shows no correlation with distance is assigned to unstructured or random interactions and amounts to 800 s^{-1} for the $M(C_2)$ isomer and to 1180 s^{-1} for the $P(C_2)$ isomer. For the $M(C_2)$ isomer, the paramagnetic center of $[Cr(edta)]^-$ is calculated to be 6.3 Å from cobalt(III) and is located close to one of the amine terminal ^1H atoms of the diamagnetic complex. A value for $K = 2.1$ M^{-1} can be estimated by assuming a correlation time for the ion pair of 8×10^{-11} s, comparable with values observed for similar species[22] where the thermodynamic stability is large enough to permit measurement. A similar orientation at 6.1 Å was found for the $P(C_2)$ isomer, and the value of $K = 0.4$ M^{-1} in this instance is smaller. However, this difference is not considered significant as the conditions for the two experiments differed slightly. The relative orientations of the two diastereomers with respect to the Cr–Co vector are shown in Figure 6.

Discussion

The reduction potential of $[Ni(H_{-1}GG)_2]^-$ is estimated to be 0.66 V (vs NHE) and qualitative comparisons suggest that while the reduction potentials for the other complexes have not been determined, they are smaller than that of the parent complex, in the range 0.66–0.34 V.[6,7] The X-ray structure of the nickel(II) complex $[Ni(H_{-1}GG)_2]^{2-}$ indicates[8,9] that it is six-coordinate with approximate C_2 symmetry forming a chiral center at nickel and with two amine nitrogen, two peptide nitrogen, and two carboxylate oxygen donors. Deprotonation of the peptide nitrogen atoms occurs with pK_a values of 9.35 and 9.95.[25] Cyclic voltammetry on the nickel(III) complex at high pH where the nickel(II) complex is fully formed shows no well-defined voltammogram, which suggests that electron transfer may be slow, perhaps the result of a structural change. Electron paramagnetic resonance spectroscopy provides some structural information about the nickel(III) form.[6] It has a compressed, distorted tetragonal geometry with the peptide nitrogens forming the unique axis. It seems likely that both amine nitrogens remain coordinated, but there is no means available to discover if both carboxylate oxygen atoms are coordinated. However, it has been suggested[7] that the ligation in the nickel(III) form is identical to that in nickel(II) for the related $[Ni(H_{-1}AibAib)_2]^-$ (AibH = 2-aminoisobutyric acid).

The complexes formed with optically active dipeptides are diastereomers and are readily separated by ion-exchange chromatography in a manner similar to that used to separate the corresponding cobalt(III) species.[13] Once formed, these complexes are optically stable and decompose without interconversion. In the case of $[Ni(H_{-1}GA)_2]^-$, the $P(C_2)$ (55%) isomer predominates slightly over the $M(C_2)$ (45%), but with $[Ni(H_{-1}AA)_2]^-$, the $M(C_2)$ (75%) dominates over $P(C_2)$ (25%). In one case, $[Ni(H_{-1}GA)_2]^-$, the single $M(C_2)$ diastereomer was obtained. Both $M(C_2)$ and $P(C_2)$ diastereomers are found with $[Co(H_{-1}GA)_2]^-$.[13]

The stoichiometry of the redox process with $[Co(edta)]^{2-}$ is 1:1, in agreement with the reduction potentials of the species involved. Below pH 10, when the nickel(III) complexes are reduced, the resulting nickel(II) complexes undergo protonation and are labile. However, no exchange of the dipeptide ligand into the coordination sphere of $[Co(edta)]^-$ was noted during the time required for product analysis. The exclusive cobalt(III) product below pH 10 is $[Co(edta)]^-$, consistent with outer-sphere electron transfer. At higher pH, however, the circular dichroism spectra of the cobalt(III) products indicate the presence of some $[Co(edta)(OH)]^{2-}$. This is noted only where the reactions involving $[Co(edta)(OH)]^{3-}$ are significant and is likely also to be the product of outer-sphere reaction of the hydrolyzed complex although inner-sphere mechanisms cannot be ruled out.

The reaction kinetics are complex, particularly the dependence on pH. Rates for the reactions of $[Co(Hedta)]^-$ and $[Co(edta)(OH)]^{3-}$ are not particularly well defined in this study and will not be discussed extensively. The reactions of $[Co(edta)]^{2-}$ are of considerable interest and occupy the focus of the present work. The initial step in the reduction of $[Ni(H_{-1}GG)_2]^-$ by $[Co(edta)]^{2-}$ is the acid-catalyzed formation of a reaction intermediate (eq 6). Both metal ion complexes are anionic and formation of the intermediate must overcome the electrostatic repulsion. The rates for this reaction, k_1, are fast and are very dependent on the nature of the bis(dipeptide)nickel(III) reactant. They decrease from 3.8×10^{10} M^{-2} s^{-1} to 1.9×10^7 M^{-2} s^{-1} as the extent of methyl substitution on the peptide backbone increases. However, the position of the substituent does not appear to have a marked effect, since the values for $[Ni(H_{-1}GA)_2]^-$ and $[Ni(H_{-1}AG)_2]^-$ are very similar. There is no evidence for general acid catalysis in the reaction so that direct H^+ transfer to a preformed intermediate may be ruled out as the rate-determining step.

It seems likely that the formation of hydrogen bonds between the amine hydrogen atoms of $[Ni(H_{-1}GG)_2]^-$ and carboxylate oxygen atoms of the $[Co(edta)]^{2-}$ complex provides the thermodynamic driving force for this adduct formation, and the acid catalysis may arise from the formation of this hydrogen-bonded structure. Alternatively, the acid catalysts may derive from isomerization of the nickel(III) complex within the ion pair. Whatever the source of the acid catalysis, it pinpoints the intermediate as one with a well-defined structure, which is critical to the electron-transfer process. Without the formation of this intermediate, the rate law indicates that, within experimental uncertainty, electron transfer is turned off.

The NMR studies with the isostructural complexes $[Co(H_{-1}AA)_2]^-$ and $[Cr(edta)]^-$ were carried out to provide some indication of the way in which $[Ni(H_{-1}AA)_2]^-$ and $[Co(edta)]^{2-}$ will interact in the intermediate. For both the $M(C_2)$ and $P(C_2)$ isomers, a picture of the dominant ion-pair structure emerges in which the paramagnetic ion approaches one of the N-terminal amine groups of the bis(dipeptide) complex (Figure 6). The separation between the two metal centers, 6.1–6.3 Å, is consistent with an intimate interaction between the complexes and is close to that measured for closest contact of space-filling models. The orientation allows strong hydrogen-bond formation between the N-terminal amine ^1H and a bound carboxylate group in $[Co(edta)]^{2-}$. In light of this orientation, it is significant that the nature of the N-terminal amino acid has the most marked effect on the rate of formation of the intermediate and on the overall rate of the electron-transfer reaction. Substituents on this amino acid will create greater steric hindrance for formation of the intermediate than substituents on the C-terminal amino acid. The orientation also suggests a site for protonation on the nickel(III)

(23) Solomon, I. *Phys. Rev.* **1955**, *99*, 559–565.
(24) Bloembergen, N. *J. Chem. Phys.* **1957**, *27*, 572–573.
(25) Martell, A. E.; Smith, R. M. *Critical Stability Constants*; Plenum: New York, 1974; Vol. 2, p 294.

complex, which would explain the acid catalysis. "Outside" protonation of the amide oxygen chromophore produces a positively charged "beacon" to direct the negatively charged carboxylate face of $[Co(edta)]^{2-}$ to the site of interaction.

The limiting second-order rate constants for the electron-transfer process, k_1k_2/k_{-1}, show a strong trend, decreasing with increasing methyl substitution on the peptide backbone, particularly at the N-terminal position. For $[Ni(H_{-1}GG)_2]^-$, the rate is over 2 orders of magnitude slower than the rate of reaction with $[Co(phen)_3]^{2+}$. Outer-sphere reactions of a number of nickel(III) complexes with these two reagents[26,27] show a similar effect which may be ascribed to the much higher electronic self-exchange rate of the $[Co(phen)_3]^{3+/2+}$ couple.[17] It is likely that both reactions of $[Ni(H_{-1}GG)_2]^-$ are in this instance outer sphere in nature. Application of the Marcus correlation[28] to the data can thus be used to elucidate the self-exchange rate of the $[Ni(H_{-1}GG)_2]^{-/2-}$ system.

The Marcus theory may be conveniently expressed[29,30] in free energy terms as eqs 12 and 13, where ΔG_{12}^* represents the free

$$\Delta G_{12}^* = \tfrac{1}{2}[\Delta G_{11}^* + \Delta G_{22}^* + \Delta G^\circ(1 + \alpha^*)] \quad (12)$$

$$\alpha^* = \Delta G^\circ/4(\Delta G_{11}^* + \Delta G_{22}^*) \quad (13)$$

energy of activation for the cross reaction, ΔG_{11}^* and ΔG_{22}^* are the corresponding terms for the self-exchange reactions, and ΔG° is the free energy change for the cross reaction. It is customary to correct these parameters for electrostatic work involved in the approach of charged reagents in the reaction medium, and this has been carried out as outlined previously.[26,29] With use of the simpler reaction of $[Co(phen)_3]^{2+}$, the self-exchange rate for $[Ni(H_{-1}GG)_2]^{-/2-}$ is calculated[31] to be ≈ 1 M^{-1} s^{-1}, which is comparable with the value of 48 M^{-1} s^{-1} for the larger $[Ni(H_{-1}AibAib)_2]^{-/2-}$ complex.[7] The rate for the reaction of $[Ni(H_{-1}GG)_2]^-$ with $[Co(edta)]^{2-}$ obtained[32] with this self-exchange rate is ≈ 0.1 M^{-1} s^{-1}, over 2 orders of magnitude slower than the rate which is observed. Such discrepancies may indicate that this particular reaction is inner sphere. However, if this reaction is outer sphere in nature, the discrepancy can equally be explained by the formation of a specific interaction between the participants in the cross reaction and is therefore completely consistent with the proposed mechanism. The magnitude of the effect suggests that $k_1/k_{-1} \approx 1$ M^{-1}, in line with the NMR results, and that $k_2 \approx 20$ s^{-1}.

The reaction stereoselectivities are also an important source of information about the interactions between the complexes. Three complexes with the $M(C_2)$ configuration have been examined (Table III). At pH 6.1, the induction appears to be dependent only on the nature of the N-terminal amino acid. For the $M(C_2)$-$[Ni(H_{-1}AG)_2]^-$ and $M(C_2)$-$[Ni(H_{-1}AA)_2]^-$ at pH 6.1, the stereoselectivities are 14.4% Λ and 14.2% Λ, respectively. The (*S*)-methyl group on the alanine to which the reductant is hydrogen bonded is the only chiral group within the binding site region. When this is absent, as in $M(C_2)$-$[Ni(H_{-1}GA)_2]^-$, the stereoselectivity is very small, 2% Λ. In the two complexes with the $P(C_2)$ configuration, $P(C_2)$-$[Ni(H_{-1}GA)_2]^-$ has a stereoselectivity of 12.5% Δ and $P(C_2)$-$[Ni(H_{-1}AA)_2]^-$ has a stereoselectivity of 5.9% Λ. In this case both N-terminal (*S*)-methyl groups and one C-terminal (*S*)-methyl group are located around the binding site region for $P(C_2)$-$[Ni(H_{-1}AA)_2]^-$ and only the C-terminal group is located for $P(C_2)$-$[Ni(H_{-1}GA)_2]^-$. Both N-terminal and C-terminal groups have an effect on the stereoselectivity. In the absence of any methyl group, a stereoselectivity around 2% Δ might be expected for the $P(C_2)$ isomers by analogy with the $M(C_2)$-$[Ni(H_{-1}GA)_2]^-$. It is interesting to note that the magnitude of the stereoselectivity observed in these reactions is of the same order as that previously observed for reactions of complementary charge that are dependent on hydrogen bonding for chiral recognition.[3,4,26] Thus, the electrostatic repulsion does not appear to be a major influence.

The pH dependence of the stereoselectivity was investigated with the almost equimolar mixture of $P(C_2)$- and $M(C_2)$-$[Ni(H_{-1}GA)_2]^-$ and the stereospecifically produced $M(C_2)$-$[Ni(H_{-1}AG)_2]^-$. In both cases, reactions run around pH 3.7 showed behavior almost identical to that observed at pH 6.1. At pH 10, however, there is a fundamental change in both systems which supports the kinetic indications of a change in the reaction mechanism. The stereoselectivity is of the same sense but is reduced in magnitude compared with that observed at lower pH. In addition, while the visible absorption spectrum of the isolated cobalt(III) product differs little from that observed at pH 6.1, the circular dichroism spectrum[21] at higher pH is indicative of a mixture of $[Co(edta)]^-$ and the quinquedentate $[Co(Hedta)OH]^-$. Again, this is consistent with a marked switch-off in reactivity in the reaction of $[Co(edta)]^{2-}$, the result of acid catalysis in the formation of the reaction intermediate, and the predominance of the reaction of $[Co(edta)OH]^{3-}$.

Finally, stereoselectivity in the reduction of the stereospecifically formed $M(C_2)$-$[Ni(H_{-1}AG)_2]^-$ by $[Co(phen)_3]^{2+}$ was investigated at pH 7.3. The reaction product, $[Co(phen)_3]^{3+}$, is optically active with a 3.3% enantiomeric excess of the Λ isomer. However, the chiral induction is transient, as racemization by self-exchange in the presence of an excess of $[Co(phen)_3]^{2+}$ takes place.[17] It is noteworthy that even though electrostatic forces are attractive in this case, the stereoselectivity is small. It may concluded that directional organizing forces such as hydrogen bonding are more effective in chiral discrimination than a general electrostatic attraction.

Acknowledgment. We thank the National Science Foundation (Grant No. CHE-9016682) for generous support of this work. Thanks are also expressed to Lisette Bauersachs, who carried out preliminary studies.

Registry No. $[Co(edta)]^{2-}$, 14931-83-0; $[Ni(H_{-1}GG)_2]^-$, 117019-42-8; $[Ni(H_{-1}GA)_2]^-$, 32270-34-1; $[Ni(H_{-1}AG)_2]^-$, 137328-51-9; $[Ni(H_{-1}AA)_2]^-$, 137253-94-2; $M(C_2)$-$[Ni(H_{-1}GA)_2]^-$, 137253-95-3; $P(C_2)$-$[Ni(H_{-1}GA)_2]^-$, 137253-96-4; $M(C_2)$-$[Ni(H_{-1}AG)_2]^-$, 137253-97-5; $M(C_2)$-$[Ni(H_{-1}AA)_2]^-$, 137253-98-6; $P(C_2)$-$[Ni(H_{-1}AA)_2]^-$, 137253-99-7; $Co(phen)_3^{2+}$, 16788-34-4; $[Co(H_{-1}AA)_2]^-$, 71179-47-0; $[Cr(edta)]^-$, 16091-77-3.

Supplementary Material Available: A list of pseudo-first-order rate constants for the oxidation of $[Co(edta)]^{2-}$ by $[Ni(H_{-1}GG)_2]^-$, $[Ni(H_{-1}GA)_2]^-$, $[Ni(H_{-1}AG)_2]^-$, and $[Ni(H_{-1}AA)_2]^-$ (Table SI) (6 pages). Ordering information is given on any current masthead page.

(26) Martone, D. P.; Osvath, P.; Lappin, A. G. *Inorg. Chem.* **1987**, *26*, 3094–3100.
(27) Lappin, A. G.; Martone, D. P.; Osvath, P.; Marusak, R. A. *Inorg. Chem.* **1988**, *27*, 1863–1868.
(28) Marcus, R. A. *Annu. Rev. Phys. Chem.* **1964**, *15*, 155–196.
(29) Brown, G. M.; Sutin, N. *J. Am. Chem. Soc.* **1979**, *101*, 883–893.
(30) Newton, M. D.; Sutin, N. *Annu. Rev. Phys. Chem.* **1984**, *35*, 437–480.
(31) The reduction potential and self-exchange rate for $[Co(phen)_3]^{3+}$ are 0.36 V and 12 M^{-1} s^{-1},[17,27] The radii of the reactants, $[Co(phen)_3]^{3+/2+}$ and $[Ni(H_{-1}GG)_2]^{-/2-}$, were estimated from space-filling models as 6.8 and 4.5 Å, respectively.
(32) The reduction potential and self-exchange rate for $[Co(edta)]^-$ are 0.37 V (Ogino, H.; Ogino, K. *Inorg. Chem.* **1983**, *22*, 2208–2211) and 2×10^{-7} M^{-1} s^{-1} (Im, Y. A.; Busch, D. H. *J. Am. Chem. Soc.* **1961**, *83*, 3357–3362). The radius of $[Co(edta)]^{-/2-}$ estimated from space-filling models is 4.3 Å.